

## NEGATIVE FIELD-EFFECT MOBILITY ON (100) Si SURFACES

F. F. Fang and W. E. Howard

IBM Watson Research Center, Yorktown Heights, New York

(Received 7 March 1966)

The surface mobility of carriers in an  $n$ -type inversion layer has been studied by field-effect experiments with metal-oxide-semiconductor structures. It was shown that at moderate fields the carriers suffer from surface scattering and the surface mobility, as measured from both field-effect mobility<sup>1</sup> and the surface Hall effect,<sup>2</sup> is reduced with increasing field.

In this Letter, we report an anomalous effect of high field ( $>10^6$  V/cm) on the field-effect mobility, which is defined as  $\mu_{F.E.} = \partial\sigma_s / \partial Q_s$ . Figure 1 shows the surface conductivity as a function of the applied normal field at 77°K. The sample is an insulating gate field-effect transistor with the surface normal to the [100] direction. The field plate is on a 1000-Å thick SiO<sub>2</sub> layer. The measuring voltage used in the surface inversion layer is about 0.01 V so that there is a negligible effect on the uniformity of the normal field. It is seen that the surface conductivity increases slower than linearly with increasing normal field at moderate fields as one would expect. At higher fields, the conductivity levels off and finally decreases with increasing field. The corresponding field-effect mobility, measured at 500 cps, is also shown in Fig. 1. The maximum surface conductivity (at  $\mu_{F.E.} = 0$ ) is at a normal field of about  $3 \times 10^6$  V/cm in the oxide. This phenomenon is very reproducible from sample to sample. Samples with different Si resistivities and different oxide thickness do not differ appreciably.

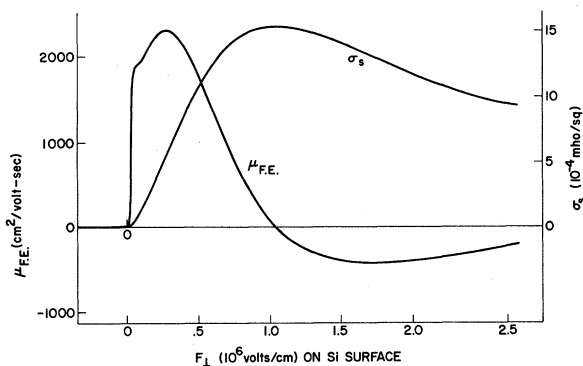


FIG. 1. Field-effect mobility and surface conductivity as a function of the normal electric field at the surface at 77°C.

ably. Samples on (111) surfaces do not show this anomaly. It is noted that at low field, the structure in the  $\mu_{F.E.}$  curve is also absent in that for (111) oriented samples, the exact shape of this structure is not very reproducible. It is also observed that the field at which the maximum  $\sigma_s$  occurs increases with temperature. For example, at 298, 77, and 4.2°K, this field is about  $6 \times 10^6$ ,  $3 \times 10^6$ , and  $2.5 \times 10^6$  V/cm, respectively. The structure at low field disappears at 4.2°K.

The surface mobility, or  $\sigma_s/Q$ , of the electrons deduced from Fig. 1 is plotted in Fig. 2, assuming that the number of surface carriers corresponds to the charge induced by the field plate.<sup>3</sup> This assumption is justified for a highly inverted surface, as is produced in these experiments.

An explanation of this unusual behavior for (100) surfaces can be offered in terms of the quantization of free-electron states in the narrow potential well which forms the channel in a field-effect device. In order to form an inversion channel on a  $p$ -type semiconductor surface, the conduction band is bent downward in energy under the influence of the electrostatic

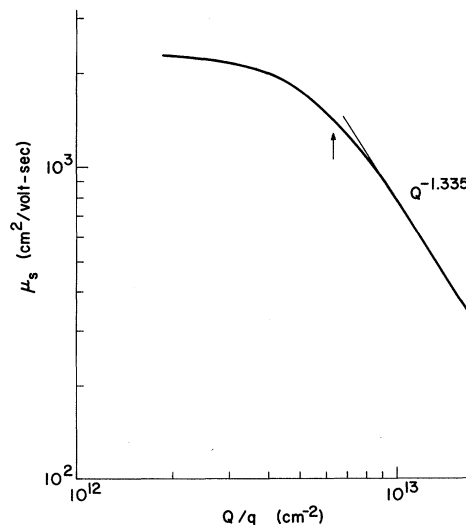


FIG. 2. Effective surface mobility as a function of the normal electric field at the surface. The arrow indicates where  $\mu_s \propto Q^{-1}$ , the onset of negative  $\mu_{F.E.}$  was observed.

field. Since the vacuum level or, in this case, the conduction band of the insulator is much higher in energy, the result is a potential well (see Fig. 3), which, depending on the semiconductor doping, may be quite narrow. "Narrow," here, means that the distance from the interface to the classical turning point for electrons of thermal energy would be small compared with an electron wavelength. It has been recognized for some years that this situation should be treated quantum-mechanically<sup>4</sup>; in fact, Handler and Eisenhour have calculated the energy levels for the light holes in a *p* channel in Ge in the presence of charge due to the heavy holes.<sup>5</sup>

The important aspect of the (100) surface, especially in contrast to the more extensively studied (111) surface, is that the six conduction ellipsoids are not equivalent in the presence of a channel field, thus the field may be expected to remove their degeneracy. In order to determine the magnitude of the splitting, we calculated the lowest energy levels, using an effective-mass Hamiltonian<sup>6</sup> and a self-consistent variational approach.

Consider the (001) surface, i.e., take the *z* direction normal to the surface. Since for Si  $m_l/m_t \approx 5$ , it is clear that the two ellipsoids whose long axes lie along the [001] direction will lie lower in energy than the other four. Further, since the additional electrostatic potential is  $\varphi = \varphi(z)$ , we can write

$$\psi(001) = \psi_0(001) \exp[i(k_x x + k_y y)]$$

and

$$E(001) = E_0(001) + (\hbar^2/2m_t)(k_x^2 + k_y^2),$$

then

$$E_0(001)$$

$$\leq -\frac{\hbar^2}{2m_t} \int \psi_0(001) \frac{\partial^2}{\partial z^2} \psi_0(001) dz - q \int |\psi_0(001)|^2 \varphi dz.$$

If the mobile charge  $Q=0$ , then  $\varphi \cong (4\pi Q_{SC}/\epsilon)z$ , where  $Q_{SC}$  is the space charge due to the ionized acceptors. As mobile charge is added, an additional contribution to  $\varphi$  is obtained from Poisson's equation

$$\nabla^2 \varphi \cong (4\pi/\epsilon)Q |\psi_0(001)|^2.$$

This approach is valid so long as the Fermi energy is less than the splitting, that is, as long as no electrons occupy the upper four min-

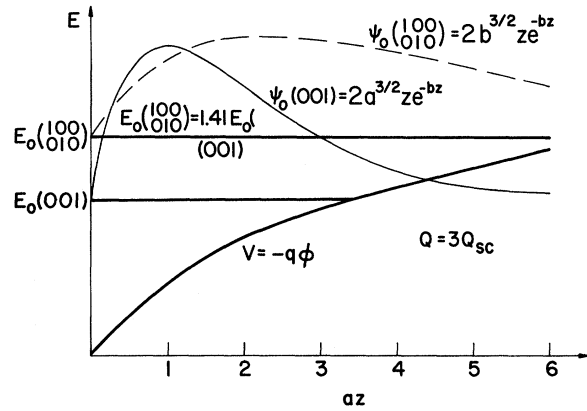


FIG. 3. Electron-energy diagram of a potential well and the ground-state eigenvalues and eigenfunctions for the two inequivalent sets of ellipsoids when  $Q=3Q_{SC}$  as an example.

ima. We have used as a trial function  $\psi_0(001) = 2a^{3/2}ze^{-az}$  and have minimized  $E(001)$  with respect to  $a$ . Having obtained the quantity  $a(Q)$  in this way, we can solve for  $E(100, 010)$  simply by substituting  $m_t$  for  $m_l$  while using the same  $\varphi(az)$ . Figure 3 shows the results for one case ( $Q=3Q_{SC}$ ). It may be interjected at this point that the extent of the wave functions obtained is consistent with the use of the effective-mass approach; that is, it extends over many unit cells. Proceeding in this way, we can show that for a given  $Q_{SC}$ , there is a  $Q$  for which the Fermi energy measured from  $E(001)$  is equal to the splitting. In our case, for  $Q/q > (3-5) \times 10^{12}/\text{cm}^2$ , one should begin populating the other four ellipsoids. In terms of gate voltage, this is approximately 10-15 V. One can calculate the two-band effective surface mobility in a rough way using the following two assumptions: (1) The mobility of electrons in the upper band is much lower than that in the lower band. This is based on the fact that both density of states and effective mass are greater for the upper ellipsoids. (2) The mobility of electrons in each band has a strong field dependence, as in a (111) surface; i.e.,  $\mu \propto Q^{-1}$  for each band (attributed to diffuse scattering in the classical case). The splitting between bands is found theoretically to increase at most as  $Q^{2/3}$ , which is the result for a constant-field well. These considerations lead to an effective surface mobility varying more strongly than  $Q^{-4/3}$ . The observed variations range from  $Q^{-1.33}$  to  $Q^{-1.42}$ . This agreement is more significant than simply obtaining a

negative field-effect mobility, which requires only that the effective surface mobility vary more strongly than  $Q^{-1}$ .

<sup>1</sup>F. Fang and S. Triebwasser, *Appl. Phys. Letters* **4**, 145 (1964); *IBM J. Res. Develop.* **8**, 410 (1964).

<sup>2</sup>A. B. Fowler, F. Fang, and F. Hochberg, *IBM J. Res. Develop.* **8**, 427 (1964).

<sup>3</sup>A recent field-effect Hall measurement by A. B. Fowler on a (100) Si surface showed that there is no significant loss of carriers due to oxide trapping at

the field where negative  $\mu_{F,E}$  was observed. We are indebted to him for making available the data before an intended publication.

<sup>4</sup>See, for example, J. R. Schrieffer, *Semiconductor Surface Physics*, edited by R. H. Kingston (University of Pennsylvania Press, Philadelphia, Pennsylvania, 1956), p. 55.

<sup>5</sup>P. Handler and S. Eisenhour, *Solid Surfaces*, edited by H. C. Gatos (North-Holland Publishing Company, Amsterdam, 1964), p. 64.

<sup>6</sup>J. M. Luttinger and W. Kohn, *Phys. Rev.* **97**, 869 (1955).

### CRYSTAL STRUCTURE OF PARA-ENRICHED SOLID DEUTERIUM BELOW THE $\lambda$ TRANSITION\*

K. F. Mucker, S. Talhouk, P. M. Harris, and David White

Department of Chemistry, The Ohio State University, Columbus, Ohio

and

R. A. Erickson

Department of Physics, The Ohio State University, Columbus, Ohio

(Received 14 March 1966)

It has recently been reported by Mills and Schuch<sup>1</sup> that the crystal structure of solid normal hydrogen undergoes a change below the temperature of the  $\lambda$  anomaly observed in the heat capacity.<sup>2</sup> Above the  $\lambda$  anomaly the solid is reported to exhibit a hexagonal close-packed structure, and below the  $\lambda$  transition this hexagonal phase changes to a face-centered cubic lattice. These results are in accord with deductions concerning the crystal structure of the solid from the infrared spectrum of normal hydrogen.<sup>3</sup>

In an earlier communication<sup>4</sup> we reported the results of neutron-diffraction studies of solid ortho and normal deuterium at 13°K. The structure of both solids is hexagonal close-packed,  $a = 3.63 \text{ \AA}$  and  $c/a = 1.61$ . We have now extended our neutron-diffraction measurements to lower temperatures and to para-enriched solids which, like normal hydrogen, exhibit anomalies in the nuclear magnetic resonance<sup>5</sup> and  $\lambda$  transitions in the heat capacities.<sup>6</sup> The neutron diffraction patterns for the para-enriched solids (para content >80%) above the  $\lambda$ -transition temperatures of the heat capacities are, within experimental error, the same as those for ortho and normal deuterium with respect to both line positions and intensities. The high-temperature form of solid deuterium is, therefore, hexagonal close-packed irrespec-

tive of the para content.

The neutron diffraction pattern of a solid deuterium sample containing 83% para species at 1.9°K is shown in Fig. 1. The experimental apparatus used in these measurements was similar to that previously used,<sup>4</sup> the deuterium being rapidly solidified in an aluminum-magnesium sponge. The enrichment in para content was accomplished by fractional desorption from a column packed with  $\gamma\text{-Al}_2\text{O}_3$ . The three diffraction patterns of Fig. 1 correspond to the background counts  $N_B$  for the cryostat at 4.2°K, trace C; the total counts  $N_T$  at 1.9°K for the cell filled with 83% para-deuterium, trace B; and the difference pattern  $N_T - pN_B$ , trace A, where  $p$  is a constant equal to 0.8 which corrects for removal of neutrons from the incident beam by the deuterium sample. The three most intense lines can be identified as the 111, 200, and 220 reflections of cubic phase. While these obey the extinction requirements of a fcc lattice with  $a = 5.084 \pm 0.004 \text{ \AA}$ , the two weak lines of pattern A in Fig. 1 appear to be real. These two lines cannot be discounted as due to random statistics or an arbitrary choice of the constant  $p$ . A calculation of  $p$  using the total cross section of deuterium yields a value of  $p \geq 0.75$ . These two weak lines have been identified as the 210 and 211 reflections of the above cubic cell, which do not obey the